Solar-powered space flight

M. H. D. Kemp
London

ABSTRACT

The aim of this paper is analyse the practicality or otherwise of solar-powered propulsion (after launch using conventional chemical rocketry) for a space vehicle's late pre-orbital trajectory phase, for orbital transfer and for post-orbital flight. We introduce a 'concept' vehicle that in principle permits the use of solar-powered propulsion in each of these stages. Some of the technical challenges that such a vehicle might face are analysed, including the problem of how to keep a large ultra-low mass optical concentrator arrangement sufficiently accurately positioned in different parts of such a trajectory.

NOMENCLATURE

$a_i(k)$ angle that tangent at k'th point on i'th mirror makes to x-axis (or 90° if $i = 0, 3$)
$a(r)$ angle that first (larger) mirror makes to x-axis at distance r from x-axis
β angle that stanchion makes to x-axis if mirror area element only has a single stanchion
B magnification of mirror pair
C_D drag coefficient of mirror arrangement
c thickness of mirror
$d_i(k)$ angle that the line from $M_i(k)$ to $M_{i+1}(k)$ makes to x-axis
E energy per unit time available for thrust
f position along (negative) x-axis of the Sun
F_D drag force per unit cross-sectional area perpendicular to the velocity vector
$F(r,\theta)$ also F_x, F_r, F_θ. Additional force (in cylindrical polar coordinates) per unit mirror area (area perpendicular to x-axis) provided by stanchions, $F_T = \sqrt{F_x^2 + F_r^2}$ = total force per unit mirror area (area perpendicular to x-axis) provided by stanchions in rotationally symmetric case, F_1, …, F_7 = component elements in equations linking F_x and F_r with T_r and T_θ
g acceleration due to gravity (assumed to be 10ms^{-2} at the surface of the Earth
$\bar{g}(t)$ effective acceleration due to thrust
h iteration increment size for mirror positioning analysis (can be positive or negative)
k iteration step counter for mirror positioning analysis
$m(t)$ mass of launcher plus propellant at time t
m' rate of change of $m(t)$ with respect to t (is negative)
$M_i(k)$ = $(m_{i,x}(k), m_{i,y}(k))$. If $i = 1$ or 2 then k'th point of i'th mirror in xy-plane. If $i = 0$ then object point of mirror pair, $(f, 0)$. If $i = 3$ then image point, (0, 0).
M mass of mirror
p upper limit on propellant ejection speed (if applicable)
$p_i(k)$ distance between $M_i(k)$ and $M_{i+1}(k)$
q_1, q_2 arbitrary real numbers (positive or negative) defining the shape of the mirror layout
r_0 radius of larger mirror
ρ density of material used to make larger mirror
ρ_α density of atmosphere
s = $\dot{\theta}/\bar{g}$, where $\dot{\theta}$ is the angular velocity of the mirror
t time from commencement of solar-powered propulsion
$T(r,\theta)$ = (T_r, T_θ). Tension per unit cross-sectional area in mirror at (x, r, θ), T_θ being the tension in the transverse direction and T_r being the tension perpendicular to this and tangential to the mirror surface. T_α = uniform tension whatever the direction (tangential to mirror) if $T_r = T_\theta$ (= T_α)
T_r' rate of change of T_r with respect to r (for mirror defined with $|m_{1,y}(0)| = 0$)
u vertically downward speed at which propellant is ejected (relative to launcher)
$v(t)$ velocity of launcher plus propellant at time t
v' rate of change of $v(t)$ with respect to t

Paper No. 2955. Manuscript received 14 February 2005, revised version received 21 September 2005, accepted 25 October 2005.

v_o orbital speed (assumed to be 7,800ms^{-1} for low Earth orbit)
w horizontal speed at which propellant is ejected (relative to launcher)
w_1, w_2 distance between consecutive points in cross-sections of first and second mirrors respectively
x, r, θ cylindrical polar coordinates corresponding to Cartesian coordinates (x, y, z)
Z a sign factor (i.e. either ±1) used in identification of mirror pair positioning

1.0 INTRODUCTION

Solar power is routinely used to provide on-board power for space vehicles. However, it is rarely used for actual propulsion purposes. Instead, nearly all space vehicles currently use chemical rocketry. This is despite solar power being plentiful in space (at least in the vicinity of the earth).

The aim of this paper is to analyse the practicality or otherwise of solar-powered space vehicles that deliberately aim to use solar power for propulsion purposes for as much as possible of a vehicle's trajectory. Almost certainly, such a vehicle would need to employ chemical rocketry in its early pre-orbital trajectory, to lift itself high enough to limit atmospheric drag. So, in practice our aim is to analyse the use of solar-powered propulsion in a vehicle's late pre-orbital trajectory phase, for orbital transfer and for any subsequent post-orbital trajectory. Ideally, we would use the same solar power collector arrangement in each phase, to minimise the mass of the propulsion system and to make the vehicle as reusable as possible.

We do this by describing a 'concept' vehicle that uses a two-mirror collector arrangement with optical characteristics that ought to be particularly attractive for this purpose. Such a vehicle would undoubtedly be quite flimsy, and some of the practical engineering challenges that this would introduce are ignored, with focus instead being on some of the more fundamental challenges that such vehicle would face irrespective of how well it was manufactured.

A major technical challenge faced by such a vehicle would be the need to keep a large thin-film mirror accurately positioned during flight. Based purely on experience to date with (relatively modest sized) optical concentrators in a zero g environment, it might be considered impractical to construct a large ultra-low mass concentrator that achieves the desired position accuracy when undergoing the appreciable accelerations applicable to any pre-orbital use of solar power. But this is not necessarily sound logic. This paper argues that it ought to be easier to achieve the desired position accuracy with the proposed vehicle design in its pre-orbital trajectory (when very approximately the vehicle might be in a roughly 1g environment) than it would be for a smaller optical concentrator in an essentially zero g environment.

Another major technical challenge is posed by atmospheric drag. Once the concept vehicle unfurled its solar power collector, atmospheric drag would be proportional to the cross-sectional area of the solar power collector (which would by necessity be large). Therefore atmospheric drag cannot be ignored except in deep space. However, careful optimisation of the flight speed and trajectory, following a conventional rocket launch to lift the vehicle above the lower atmosphere, may be able to mitigate this problem rather more than might be expected, because atmospheric drag is also proportional to the square of the vehicle's velocity.

2.0 STRUCTURE OF PAPER

The optimal use of propellant for a solar-powered vehicle differs significantly from that applicable with a conventional chemical rocket in any pre-orbital phase. Typically, before orbit is reached, it is optimal for a chemical rocket to accelerate as fast as possible (subject to any limits imposed by the engineering of the vehicle itself). In contrast, a more leisurely approach is optimal for a solar-powered rocket, because the longer the flight time the more energy the solar power collector can collect. We explore this further in Sections 3 and 4 by analysing the theoretical power requirements of a hypothetical solar-powered vehicle for a series of increasingly sophisticated flight trajectory scenarios. Section 3 ignores atmospheric drag. Section 4 extends the analysis to include the impact of atmospheric drag.

In Section 5 we consider how large a proportion of total payload the solar power collector element of the vehicle might need to be to deliver the power requirements identified in Sections 3 and 4, if we make the unrealistic assumption that all incident solar energy is converted with 100% efficiency into thrust. We introduce a two-mirror collector arrangement that appears to have close to optimal optical characteristics for this purpose.

Section 6 considers the propulsion approaches that are likely to be the most efficient when combined with the sorts of solar collectors proposed in Section 5. At least in earlier trajectory phases, solar thermal propulsion seems likely to be the most attractive approach, although propellant-less solar sail propulsion methodologies may be favoured post orbital transfer.

Sections 7 and 8 consider some of the other practical challenges that such a vehicle would face. Section 7 considers in some detail the potential difficulties involved in keeping a large ultra-thin mirror sufficiently accurately positioned, whilst Section 8 covers some of the other issues, including the need to ensure that the solar collector does not foul the engine exhaust plume of a solar thermal engine.

Finally, Section 9 contains some concluding remarks applicable to the concept vehicle considered in the paper and to solar-powered space propulsion more generally.

3.0 THE POWER REQUIRED FOR A SOLAR-POWERED VEHICLE TO REACH ORBIT IF ATMOSPHERIC DRAG IS IGNORED

For solar-powered flight, E can be assumed to be constant, unlike with chemical rocketry where E is proportional to propellant used per unit time. In this section we ignore atmospheric drag even though this assumption is obviously unrealistic. In Section 4 we discuss the impact of atmospheric drag.

In each case we will generally wish to work out how to minimise E per unit $m(T)$, since all other things being equal this is equivalent to minimising the area of the solar power collector per unit final payload and hence presumably the mass of the collector. The optimal approach will in turn depend on the choice of $E/m(0)$, and therefore by implication also on the ratio of $(m(0) - m(T))/m(T)$, i.e. on the ratio of propellant mass to vehicle plus payload mass.

Consider first a hypothetical scenario where we launch using solar-powered propulsion from the surface of the earth into earth orbit. One possible way of estimating the power requirements of such a vehicle would be to assume that we would accelerate vertically upwards until we reached orbital velocity. In these circumstances (which would in fact fail to result in the vehicle reaching orbit), $w = 0$ and the following equations apply, derived from conservation of energy and momentum:

$$E = -\frac{1}{2}m'u^2 \quad m(g+v') = -um'$$
$$\Rightarrow m' = -2\frac{E}{u^2} \quad v' = -g - \frac{um'}{m} \qquad \ldots (1)$$

If, say, u = 5,000ms^{-1} then flight metrics for various ratios of $E/m(0)$ including the power required per unit 'lifted' mass (i.e. mass of vehicle and engine at the end of the trajectory, but not propellant) and the propellant to lifted mass ratios are as per Table 1.

These results do not initially look encouraging. The high

https://doi.org/10.1017/S0001924000000956 Published online by Cambridge University Press

Table 1
Flight characteristics to reach v_o for a range of $E/m(0)$, if propellant is ejected vertically downwards at constant speed u = 5,000ms^{-1}

$E/m(0)$ (kWkg^{-1})	Ratio of propellant to lifted mass	E (kW per kg lifted mass)	Flight time to reach v_o (s)	Maximum acceleration (ms^{-2})
150	4·8	872	69	316
100	5·3	625	105	228
50	6·6	379	217	137
40	7·6	342	276	123
30	9·2	307	376	110
25	11·2	305	459	109
20	14·6	313	585	112
15	23·3	364	799	132

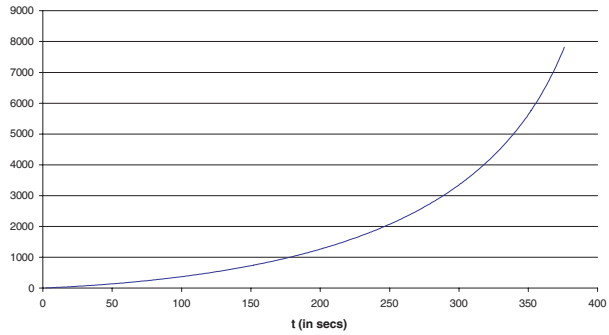

Figure 1. Plot of vehicle velocity and mass as a function of time, if propellant ejected at a constant speed vertically downwards, if $E/m(0)$ = 30kWkg^{-1}.

maximum acceleration arises because the rate of acceleration rises with time, see Fig. 1 for one of the above $E/m(0)$.

However, the required power per unit final mass falls considerably if u can vary, as does the maximum acceleration. The optimal choice of u with this sort of trajectory is to maximise v'/m' which occurs when $u = E/mg$. Flight metrics for various ratios of $E/m(0)$ using this approach are set out in Table 2. The acceleration v' experienced by the vehicle is constant throughout the flight (and equal to g), see Fig. 2.

Table 2
Flight characteristics to reach v_o for a range of $E/m(0)$, if propellant is ejected vertically downwards at optimally varying speeds

$E/m(0)$ (kWkg^{-1})	Ratio of propellant to lifted mass	E (kW per kg lifted mass)	Flight time to reach v_o (s)	Maximum acceleration (ms^{-2})
100	1·6	256	780	10
50	3·1	206	780	10
30	5·2	186	780	10
15	10·4	171	780	10
10	15·7	167	780	10
8	19·6	165	780	10
6	26·1	163	780	10

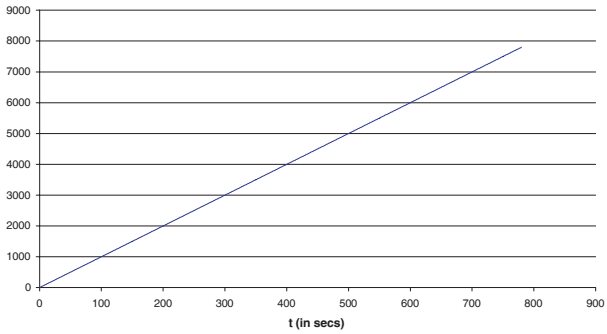

Figure 2. Plot of vehicle velocity as a function of time, if propellant ejected at a constant speed vertically downwards, if $E/m(0)$ = 30kWkg^{-1}.

Better still is to accelerate horizontally. Indeed, this approach appears to be the optimal way of reaching orbit (if we constrain the vertical velocity not to be negative). The faster the horizontal speed, the greater the centrifugal effects offsetting gravity (which of course completely offset the downward pull of gravity when orbit is reached); the effective downward acceleration becomes $g(1–v^2/v_o^2)$ rather than g. We would therefore eject propellant out at an angle that just counteracts this downward acceleration and we would choose w to maximise $–v'/m'$, so:

$$E = -\frac{1}{2}m'\left(u^2+w^2\right) \quad m.v' = -w.m'$$

$$m.g.\left(1-\frac{v^2}{v_o^2}\right) = -u.m'$$

$$\Rightarrow -v'/m' = w/m$$

$$E = \frac{1}{2}mg\frac{\left(v_0^2-v^2\right)}{v_0^2}\frac{\left(u^2+w^2\right)}{u} \qquad \ldots (2)$$

$$\Rightarrow w^2 = \frac{2E}{mg}\frac{v_0^2}{\left(v_0^2-v^2\right)}u - u^2$$

$$\Rightarrow w \text{ is maximised when } \quad u = \frac{E}{mg}\frac{v_0^2}{\left(v_0^2-v^2\right)}$$

$$\Rightarrow m' = -\frac{m^2g^2}{E}\frac{\left(v_o^2-v^2\right)^2}{v_o^4}$$

$$\text{and} \quad w = u = \frac{E}{mg}\frac{v_o^2}{\left(v_o^2-v^2\right)} \qquad \ldots (3)$$

Flight metrics for various ratios of $E/m(0)$ using this approach are in Table 3 (in theory u and w would rise without limit and the vehicle would only asymptotically reach orbit if it followed these formulae precisely). The maximum acceleration would now be at the start of the flight, see Fig. 3. It is optimal to eject propellant at 45° to the vertical.

More plausible, for reasons set out below, would be to place an upper limit on the propellant ejection velocity of p = 10,000ms^{-1}. The optimal approach is as above until this ejection speed is reached. Thereafter you would again choose w to maximise v'/m', so:

$$E = -\frac{1}{2}m'\left(u^2+w^2\right) \quad p^2 = u^2+w^2$$

$$m.v' = -w.m' \quad mg\left(1-\frac{v^2}{v_o^2}\right) = -um' \qquad \ldots (4)$$

https://doi.org/10.1017/S0001924000000956 Published online by Cambridge University Press

Table 3
Flight characteristics to reach orbit for a range of $E/m(0)$, if propellant is ejected at optimal speeds and the vehicle accelerates horizontally

$E/m(0)$ (kWkg^{-1})	Ratio of propellant to lifted mass	E (kW per kg lifted mass)	Flight time to reach v_o (s)	Maximum acceleration (ms^{-2})
100	0·5	152	> 2,000	10
50	1·0	102	> 2,000	10
30	1·7	82	> 2,000	10
15	3·5	67	> 2,000	10
10	5·2	62	> 2,000	10
8	6·5	60	> 2,000	10
6	8·7	58	> 2,000	10

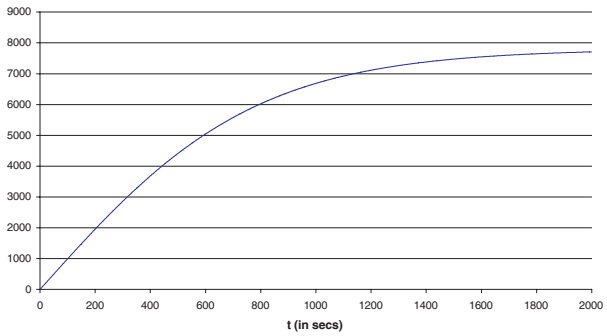

Figure 3. Plot of vehicle velocity as a function of time, if vehicle accelerates horizontally and propellant is ejected at optimal speeds and angles, if $E/m(0)$ = 10 kW kg^{-1}.

$$\Rightarrow m' = -\frac{2E}{p^2} \quad \text{and} \quad w = \left(p^2 - m^2 g^2 p^4 \frac{\left(v_o^2 - v^2\right)^2}{4 v_o^4 E^2} \right)^{1/2} \qquad \ldots (5)$$

Flight metrics for various ratios of $E/m(0)$ using this approach are in Table 4. In such a trajectory, $\bar{g} = \sqrt{v'^2 + g^2 \left(1 - v^2/v_0^2\right)^2}$ is the effective thrust acceleration experienced by the vehicle. This acceleration is relatively modest in relation to that typically applicable to chemical powered rocketry (although much higher than for previously suggested solar-powered vehicles). If $E/m(0)$ = 10kW kg^{-1} then $\bar{g}$ starts at $\sqrt{2}g \approx 1{\cdot}4g$, falls to approximately 0·8g somewhat after half-way through the flight into orbit, and then increases again to about 1·4g when orbital velocity is reached, see Fig. 4. Once the propellant ejection speed reaches its upper limit, the optimal ejection angle ceases to be 45° to the vertical and changes (seemingly uniformly through time) until it becomes horizontal when orbit is reached. In practice, it may be preferable to continue to eject propellant in a direction opposite to that of the Sun, see later. Given the relatively short flight time involved this would imply an approximately constant ejection angle throughout flight, which if adopted would increase modestly the required power per unit lifted mass, but would also result in a somewhat higher initial orbit.

The Earth is the largest of the inner planets and therefore the most challenging in terms of the required E to reach orbit. Even though Mars is circa 1·524 times as far away from the Sun as the Earth, its smaller size and therefore lower surface gravity and orbital velocity more than compensate for the smaller amount of solar power available per unit area in its vicinity, see Fig. 5. The same also appears to be true for all but the largest moons of Jupiter and Saturn even though they are considerably further away from the Sun.

Table 4
Flight characteristics to reach orbit for a range of $E/m(0)$, if propellant is ejected at optimal speeds (subject to an upper limit of 10,000ms^{-1}) and the vehicle travels horizontally

$E/m(0)$ (kWkg^{-1})	Ratio of propellant to lifted mass	E (kW per kg lifted mass)	Flight time to reach orbit (s)	Maximum acceleration (ms^{-2})
100	1·3	227	280	45
50	1·6	131	540	26
30	2·3	100	669	20
15	4·2	79	774	16
10	6·2	72	813	14
8	7·7	69	829	14
6	10·1	67	845	13

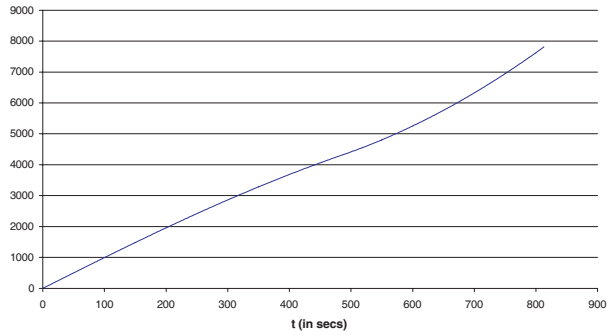

Figure 4. Plot of vehicle velocity and mass as a function of time, if propellant ejected at optimal speeds (subject to an upper limit of 10,000ms^{-1}) and angles to the vertical, if $E/m(0)$ = 10 kW kg^{-1}.

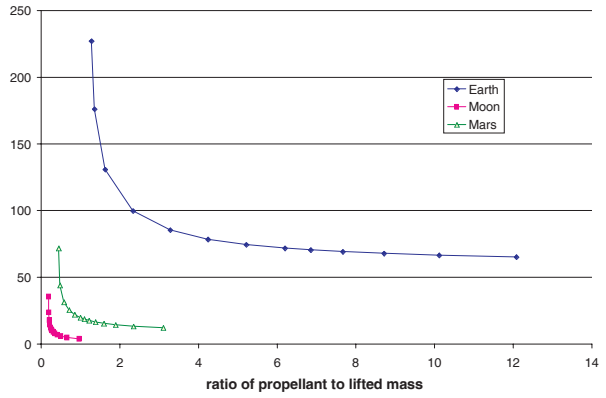

Figure 5. Values of E (for different propellant to lifted mass ratios), assuming vehicle travels horizontally and with propellant ejected at optimal speeds (subject to an upper limit of 10,000ms^{-1}) and optimal angles, for the Earth, Moon and Mars.

https://doi.org/10.1017/S0001924000000956 Published online by Cambridge University Press

Table 5
Impact of atmospheric drag at different altitudes

Altitude above Earth's surface (km)	Approximate atmospheric density (kg m^{-3})	Approximate velocity (ms^{-1}) below which drag would be below 0·1g for arrangements with mass 5g m^{-2}
0	1·2	0·06
50	$1·0 \times 10^{-3}$	1·9
100	$5·0 \times 10^{-7}$	88
150	$2·2 \times 10^{-9}$	1,334
200	$3·0 \times 10^{-10}$	3,587
300	$3·1 \times 10^{-11}$	11,127
500	$1·8 \times 10^{-12}$	46,512
800	$6·7 \times 10^{-14}$	239,840

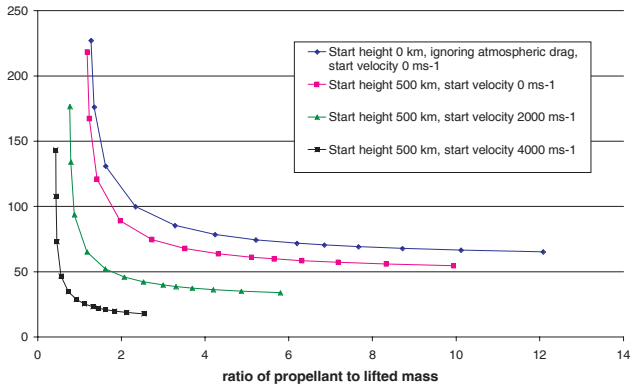

Figure 6. Values of E (for different propellant to lifted mass ratios), assuming vehicle travels horizontally with propellant ejected at optimal speeds (subject to an upper limit of 10,000ms^{-1}) and angles, if chemical rocketry is used to launch the vehicle above the Earth's atmosphere and to impart initial horizontal velocity.

4.0 TAKING INTO ACCOUNT ATMOSPHERIC DRAG

The most obvious way of overcoming air resistance early on in the flight is to use a chemical rocket to lift the vehicle above the atmosphere before then deploying the solar collector and commencing solar-powered flight.

It is worth exploring how far up is 'above' in this context. We might model the drag force per unit cross-sectional area perpendicular to the velocity vector as $F_D = 0·5\ C_D/\rho v^2$. C_D is likely to be near its maximum value of 2·6, given the shape of the mirror layout, which means that $F_D = 1·3\rho v^2$. If we assume that the collector has a mass per unit surface area perpendicular to the velocity vector of, say, 5g m^{-2} (see later), and we ignore any other contributor to the mass of the vehicle, then Table 5 shows the maximum speed (at different altitudes) at which the vehicle can travel if we want the drag deceleration to be no more than, say, 1ms^{-2} (i.e. 0·1g) We have here used atmospheric densities derived from Kaye & Laby[1] (above 30km the edition quoted in the References does not directly quote densities, so these have been estimated by applying the Gas Law to data that is quoted there, high precision not being particularly relevant for our purposes here):

At an altitude of, say, 500km (or above), the atmospheric drag that the vehicle would experience is likely to be negligible in relation to any of the accelerations envisaged by trajectories described in the previous section, even if the vehicle was travelling at close to orbital velocity. At this altitude the pull of gravity is also somewhat less than at the surface of the earth, as is the orbital velocity. Lower values of E per unit lifted mass will then suffice to reach orbit having first reached this altitude with chemical rocketry, particularly if we also use the initial chemical rocket stage to impart horizontal velocity, see Fig. 6. This might bring the required mirror mass closer to what might be within current technological capability.

Of course, the faster the vehicle reaches before it starts using solar-powered propulsion the greater would be the chemical propellant that it would need to reach this speed. But it is interesting to note that a liquid hydrogen/liquid oxygen chemical rocket as used by, say, the NASA Space Shuttle accelerating from 4,000ms^{-1} to the orbital velocity at this height (circa 7,600ms^{-1}) would itself require propellant of at least circa 1·2 times the lifted mass in this stage (if the rocket had a specific impulse of 450 s). This multiple is not dissimilar to that applicable to an equivalent solar-powered vehicle, if E were of the order of 25kW kg^{-1}.

It might be practical to start solar-powered propulsion at an altitude materially below 500km (although clearly not from ground level) if the rate of ascent was carefully optimised and if the vehicle only started to acquire appreciable horizontal velocity after it had reached a suitable altitude. It might even be possible for this lower starting altitude to be reached via methods over than conventional rocketry, e.g. by use of air-breathing engines or ultra-high altitude balloons. These possibilities are not explored further in this paper.

5.0 CREATING ULTRA-LIGHTWEIGHT SOLAR POWER CONCENTRATORS

The above analysis suggests that to make a significant contribution to any pre-orbital trajectory the vehicle would need to collect at least, say, circa 20 – 100kW kg^{-1} of solar energy. How practical is this?

The solar power incident on each 1m^2 perpendicular to the Sun's rays in the vicinity of the earth (i.e. the solar constant) is roughly 1·37 kW. So if the collector were wholly perpendicular to the Sun's rays and conversion of solar energy to thrust were 100% efficient then a power requirement of 20 – 100kW kg^{-1} would equate to 15 – 73m^2 per unit lifted mass.

Over the last few years there have been substantial advances in potential fabrication of giant ultra-low mass mirrors, principally driven by a renewed interest in solar sail technology. According to NASA[2], conventional light solar sail film has comprised of 5-micron thin aluminised Mylar with a thin film aluminium layer (approximately 100nm thick) deposited on one side to form a mirror with 90% reflectivity, weighing circa 7g m^{-2}. The solar sail that Team Encounter[3] is planning to launch is reported to have a mass of less than 4g m^{-2} (including payload). 15 – 73m^2 of a 100% reflecting 5g m^{-2} mirror would weigh only 0·08 – 0·37kg, implying that, in theory, it ought to be possible for such a mirror to lift itself into orbit with some payload to spare, following use of chemical rocketry to lift the vehicle to a height at which atmospheric drag becomes small.

We next identify a way of concentrating sunlight by using mirrors of the sort now being developed for solar sails. Ideally the mirrors should:

(a) Concentrate the sunlight by as much as possible. This should reduce the mass of any means of converting the sunlight into usable thrust and increase conversion efficiency;

(b) Have a surface area as little as possible more than the collector area perpendicular to the Sun's rays; and

(c) Be dragged 'behind' the vehicle (but without fouling propellant ejection), to enhance the stability of the vehicle in flight.

https://doi.org/10.1017/S0001924000000956 Published online by Cambridge University Press

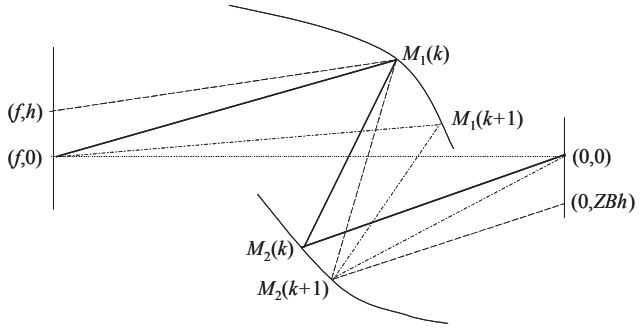

Figure 7. Schematic diagram illustrating derivation of mirror pair cross-sections.

We concentrate on rotationally symmetric aplanatic two mirror arrangements as certain of these exhibit all of the above characteristics. For those readers not familiar with optical theory, 'aplanatic' in this context in effect means 'creates a sharp focus'. Optical theory requires aplanatic arrangements involving strong magnification over a wide range of angles to have layouts that satisfy the so-called sine criterion[4]. The cross-sections can be iteratively determined as follows, see also Fig. 7:

(*i*) At the k'th iteration, a light ray starting at exactly the object point, (f, 0), should go through the image point, (0, 0), after striking the first mirror at $M_1(k)$ and the second mirror at $M_2(k)$, say.

(*ii*) We arrange for $M_2(k+1)$ both to lie on the tangent to $M_2(k)$ and if a light ray starts at (f, h), strikes the first mirror at $M_1(k)$ and the second mirror at $M_2(k+1)$ for the ray then to pass through (0, ZBh), h small (positive or negative). We identify the position of $M_1(k+1)$ in a like fashion but so that if a light ray starts at (f, 0), strikes the first mirror at $M_1(k+1)$ and the second mirror at $M_2(k+1)$ then it passes through (0, 0). In the limit as $h \to 0$, the layout is then image forming and if the correct choice of Z is made (see later) then the mirror pair is aplanatic (of order 1).

This can be mathematically re-expressed as follows[5,6]. We have for $i = 0, 1, 2$:

$$p_i = \sqrt{\left(m_{i+1,x} - m_{i,x}\right)^2 + \left(m_{i+1,y} - m_{i,y}\right)^2}$$
$$d_i = \text{Arctan}\left(\frac{m_{i+1,y} - m_{i,y}}{m_{i+1,x} - m_{i,x}}\right) \quad \ldots (6)$$

As the light rays are being deflected by reflection, we also have for $i = 1, 2$:

$$a_i = \frac{d_i}{2} + \frac{d_{i-1}}{2} \quad \ldots (7)$$

We choose seed values of $m_{i,x}(0)$ and $m_{i,y}(0)$ (for $i = 1$ and 2) so that the resulting mirror layout satisfies the sine criterion. For a far away source (e.g. $f = -10^9$) we can without loss of generality set $B = 1/p_0(0)$. The sine criterion is then satisfied if:

$$m_{1,y}(0) = \pm \frac{m_{2,y}(0)}{\left(m_{2,x}(0)^2 + m_{2,y}(0)^2\right)^{1/2}} \quad \ldots (8)$$

We can iterate either from shallower angles to more oblique angles, or vice versa. We can switch between the two by using as seed values later iterated results and reversing the sign of h. So without loss of generality (and if we wish to have the maximum possible angle span) we can iterate from highly oblique angles, choosing $m_{2,x}(0)$ equal to a small number close to zero, say 10^{-9}, and choosing $m_{1,x}(0) = q_1$ and $m_{2,y}(0) = q_2$, where q_1 and q_2 are arbitrary real numbers (positive or negative). Then $m_{1,y}(0)$ would need to be ± 1 for the initial parameters to satisfy the sine criterion. Without loss of generality we can choose $m_{1,y}(0)$ to be -1. Given these initial seed conditions different layouts arise depending on whether h is positive or negative. The choice of the sign of Z is made so that the sine criterion remains satisfied as k changes. Only one choice will work depending on the layout, for the two-mirror layout being analysed here, and if $m_{1,y}(0) = -1$, then the correct choice seems to be $Z = sgn(m_{2,y}(0))$

We iteratively update the values of $M_i(t)$ as follows for a small h

$$M_i(k+1) \equiv \begin{pmatrix} m_{i,x}(k+1) \\ m_{i,y}(k+1) \end{pmatrix} = M_i(k) + w_i(k) \begin{pmatrix} \text{Cos}(a_i(k)) \\ \text{Sin}(a_i(k)) \end{pmatrix} h \quad \ldots (9)$$

where as deflection occurs by reflection:

$$w_1 = -ZB\frac{p_1 \text{Sin}(a_3 - d_2)}{p_2 \text{Sin}(a_1 - d_1)} \quad w_2 = \frac{p_1 \text{Sin}(a_0 - d_0)}{p_0 \text{Sin}(a_2 - d_1)} \quad \ldots (10)$$

We end the iteration no later than when light rays cease to be able to pass freely through the mirror arrangement, once the cross-sections have been rotated around the x-axis to produce the complete three-dimensional mirror surfaces.

Each of the signs of q_1, q_2 and h can be either positive or negative leading to eight possible two mirror layouts. In six of the eight cases there is a discontinuity in the feasible angle ranges of rays striking the image plane when we change the value of abs(q_2) from slightly below 1 to slightly above 1[5]. Thus there are 14 possible overall layout types, whose optical characteristics can be summarised for our purposes by the following metrics:

- **effective aperture area factor** = area of first mirror perpendicular to Sun's rays, expressed as a proportion of the maximum possible were the angle span of rays falling onto the image plane to be the complete range from wholly oblique to exactly perpendicular to the image plane. The higher this is, the closer to the thermodynamic upper temperature limit such a concentrator can approach.
- **mirror surface area factor** = the total surface area of the two mirrors combined as a multiple of the effective aperture area. The closer this is to 1, the less is the mirror surface area required per unit of power delivered, and therefore the higher the power per unit mass that the concentrator can deliver.
- **aberration factor** = average maximum second order aberration for sunlight in the vicinity of the earth (i.e. for a far away source subtending approximately a semi angle of 0·267°)[6]. The lower this is, the closer the mirror pair can get to the thermodynamic upper limit when concentrating sunlight (without resorting to off-axial adjustments[6]).

The most effective layouts from our perspective appear to arise if q_1 is positive, q_2 is negative (between -1 and 0) and h is negative[5]. Figure 8 shows such a layout, if iterated to its extremities, derived from $q_1 = 2$, $q_2 = -0{\cdot}2$ and sgn(h) = -1. The darker lines are cross-sections of the mirrors themselves, and the lighter lines are the paths of light rays from the object to the image passing through extremities of the available iterative process. This layout has an effective aperture area factor of 96%, a mirror surface area factor of 1·03 and an aberration factor of 0·059. It avoids having any of the rays of sunlight crossing the positive x-axis. This is a desirable feature, as ideally propellant would be ejected along approximately this axis, see later.

https://doi.org/10.1017/S0001924000000956 Published online by Cambridge University Press

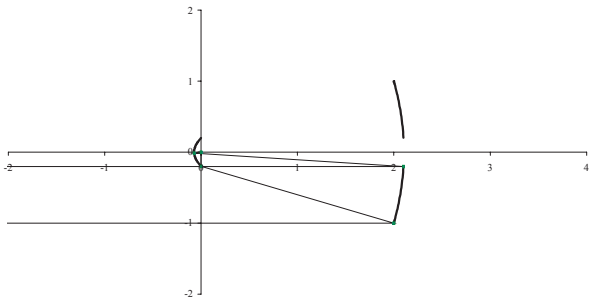

Figure 8. Mirror layout arising from $q_1 = 2$, $q_2 = -0{\cdot}2$ and $sgn(h) = -1$.

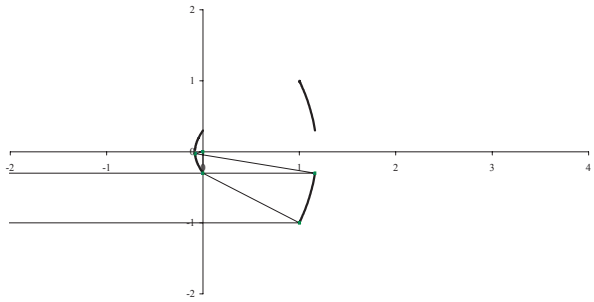

Figure 9. Mirror layout arising from $q_1 = 1$, $q_2 = -0{\cdot}3$ and $\mathrm{sgn}(h) = -1$.

A possible disadvantage of choosing the above values of q_1 and q_2 is that the larger mirror is some way away from the image point, which would increase the mass of wires joining the mirror to the main vehicle body. If instead we use $q_1 = 1$ and $q_2 = -0.3$ then the mirror layout is as shown in Fig. 9 and the main mirror would be nearer to the focal point (i.e. the origin) for a fixed collector area. Three-dimensional perspectives of this layout are shown in Fig. 10. The average aberration factor improves to 0·020. However, the aperture area factor falls to 91% and the mirror surface area factor rises to 1·13.

6.0 IDENTIFYING AN EFFICIENT MEANS OF CONVERTING CONCENTRATED SUNLIGHT INTO THRUST

The highest specific impulses currently available (other than via solar sails) involve gridded ion engines and propellant ejection speeds of circa 40,000ms^{-1}[7]. Limiting the ejection speed to 40,000ms^{-1} increases the required power per unit final mass (versus the no limit case) only very modestly. However, the conversion efficiency of sunlight into electricity is unlikely to be much above, say, 25 – 30%, and the conversion efficiency of electricity into thrust is unlikely to be much above 60%[7]. There would probably also be other components of the energy conversion process that might add significantly to the launcher mass (e.g. the power converter).

More promising is solar thermal propulsion[7]. Conceptually, all one needs is a slab with a high melting point and good thermal conductivity placed at the focal point of the layout and heated by the concentrated sunlight. Into the slab would be injected at high pressure some suitable liquid or gas (probably liquid hydrogen, given its low molecular mass and therefore high potential specific impulse). The H_2 would be vaporised by the intense heat of the slab, generating thrust probably by being expelled through narrow outlets (akin to the throats of a chemical rocket) and then expanding through suitable rocket shaped nozzles. Reducing the flow of propellant through the engine increases the engine temperature and hence the propellant ejection speed essentially continuously (up to some upper limit defined by the propellant and by the engine's maximum operating temperature). Thus it should be relatively simple to achieve the continuously varying optimal propellant ejection speed so helpful in keeping down the required collector area per unit mass lifted into orbit.

Solar thermal propulsion has been proposed for the Solar Orbit Transfer Vehicle (SOTV)[7]. The SOTV aimed to use solar thermal propulsion to move a payload from lower Earth orbit to geostationary orbit over circa 15 – 30 days, delivering a low thrust but with a high specific impulse (750 – 800 seconds, *versus* the circa 450 delivered by a liquid hydrogen/liquid oxygen chemical rocket as used by, say, the NASA Space Shuttle). The SOTV envisaged concentrating sunlight using parabolic mirrors into a cavity in which hydrogen gas was heated to circa 2,300K. The resulting expansion of the hydrogen gas would provide the thrust, the parabolic mirrors being reused in conjunction with a thermionic power converter to provide power to the payload after reaching geostationary orbit.

The two mirror layouts proposed above are imaging and can

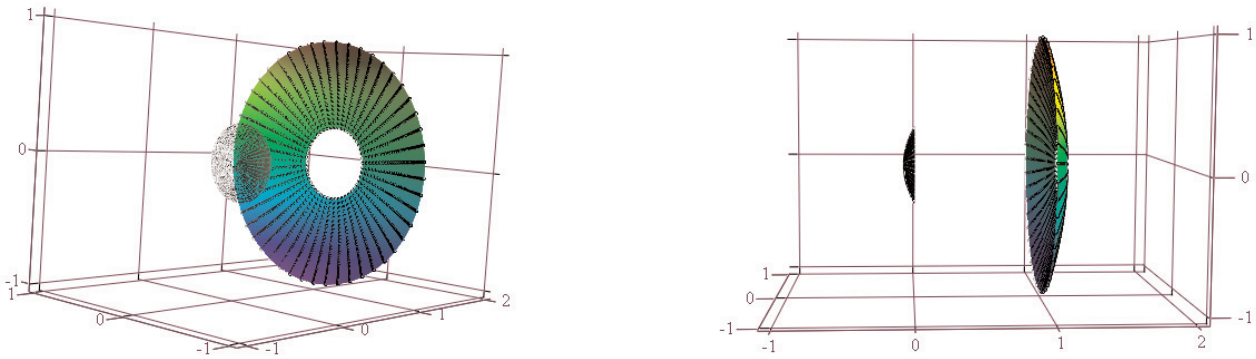

Figure 10. Three-dimensional perspectives of mirror layout arising from $q_1 = 1$, $q_2 = -0{\cdot}3$ and $\mathrm{sgn}(h) = -1$.

https://doi.org/10.1017/S0001924000000956 Published online by Cambridge University Press

therefore be used to provide power (or communications) in the same manner as the mirrors proposed for the SOTV. They also offer the following advantages over those proposed for the SOTV:

(a) In principle they can deliver temperatures as high as circa 5,900K, i.e. the temperature of the Sun's photosphere (the Second Law of Thermodynamics implies that you cannot concentrate black body radiation such as sunlight to a temperature greater than the temperature of its source). However, this temperature exceeds the highest melting points of any elements, which are those of tungsten, circa 3,680K, and carbon, circa 3,800K, and so in practice it would be necessary to limit the temperature reached to, say, circa 3,700K. Operating at circa 3,700K, the specific impulse a solar thermal engine could provide, using hydrogen as propellant, rises to about 1,000 seconds (equivalent to a propellant ejection speed of about 10,000ms^{-1}). By 'operating at circa 3,700K' we mean that the propellant is heated to this temperature in what would otherwise in a conventional chemical rocket be its combustion chamber. It is assumed that the expelled propellant would then pass through a rocket throat (in much the same manner as gasses expelled by a conventional rocket engine do), and would then experience the same sort of adiabatic cooling traversing the rocket nozzle as happens in a conventional rocket engine.

(b) They would reduce the area onto which the sunlight is concentrated, which reduces the amount reradiated away and improves overall energy efficiency. In the vicinity of the earth, the proposed mirror layouts would concentrate sunlight onto a circle with a radius circa 215 times smaller than the overall collector radius (and hence circa 46,000 times smaller in area). When operating at 3,700K approximately 15% of the incident sunlight falling onto such a solar thermal engine would then be reradiated away. If, say, the propellant from a solar thermal rocket left the rocket nozzle at a temperature of 1,000K then the thermodynamic efficiency of the engine would be subject to a thermodynamic upper limit of around (3,700 – 1,000)/3,700 = *c*.73%, but it would seem unlikely that the net conversion efficiency of the energy in the sunlight to thrust would exceed say 40%, taking into account other potential energy losses (although see later). For comparison, the combusted fuel in the Space Shuttle's main booster engine apparently reaches a temperature of at least 2,000K in its combustion chamber, but leaves the end of its rocket nozzle at *c*. 900K.

(c) They can be reused post reaching (high) orbit as a solar sail[5], either by:

Parabolic mirrors can only concentrate to circa one-quarter of this thermodynamic upper limit[8], and hence to about a 30% lower temperature (although in combination with further lenses they can get closer to the thermodynamic upper limit). This would still mean that they would be subject to the same circa 3,700K limit referred to above; the main difference therefore is that their collector surface area would be larger, making them less efficient overall.

(*i*) No longer having the Sun's rays parallel to the axis of symmetry, so that the larger mirror no longer focuses the sunlight onto the smaller mirror but deflects it in a different direction as per a traditional single mirror solar sail, or

(*ii*) By keeping the Sun's rays parallel to the axis of symmetry of the vehicle, but then putting a third small mirror at the focal point of the arrangement (instead of the solar thermal engine) and using that third mirror to deflect the sunlight in the direction as desired as per (*i*). This third mirror might most conveniently be parabolic, as then if it is suitably positioned the deflected rays would be deflected in tolerably similar directions, even though they would be approaching the focal point from a wide range of angles. This approach is more complex than a traditional single mirror solar sail, but should in principle be modestly more efficient per unit mirror mass[5]. However, it may be difficult to maintain the positioning with sufficient accuracy, see later.

Reaching a high orbit before switching to a solar sail is necessary because even at an altitude of, say, 500km atmospheric drag is still significant in the context of the very small thrust that a solar sail might provide.

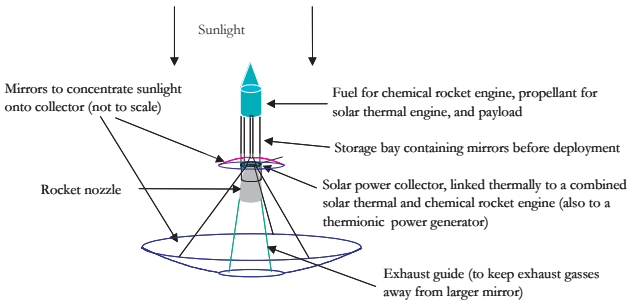

Figure 11. Schematic drawing of mirror layout used for solar thermal propulsion.

If we assume a 40% conversion efficiency of solar power into thrust and a mirror surface area factor of 1·1 then the mirror masses per unit lifted mass rise by a factor of around three. A schematic diagram of such a vehicle, not drawn to scale, is set out in Fig. 11 (the same diagram could apply in solar sail mode as per (*c*)(*i*) but with the Sun's rays now no longer parallel to the axis of symmetry). Please note that there might in practice be more than three wires connecting the main mirror to the rest of the vehicle superstructure, see later.

One worry might be that it would be impossible to create a slab of low enough mass able to cope with the relevant heat transfer involved with a solar thermal engine. Careful design is likely to be needed to maximise heat transfer whilst minimising mass and maximising structural rigidity, but it should not be impossible. The solar power concentrated onto the slab would be approximately 46,000 × 1·37kWm^{-2} = 63 × 10^{6}kWm^{-2}. If we assume the slab is made of tungsten and it has a thermal conductivity of circa 100Wm^{-1} K^{-1} at the relevant temperature (Kaye and Laby[1] have a figure of 119 at 973K, but reducing as temperature rises) and heat transference takes place through a slab with effective thickness for this purpose of 1mm then the temperature differential involved would be 630K. Tungsten has a tensile strength of 1,500 – 3,500MPa. Even if all of the force from the rocket thrust is borne by the slab, the pressure should in theory (for the $E/m(0)$ = 10kW kg^{-1} case considered in Table 4) be only at most around roughly $(1 + 6{\cdot}2) \times \sqrt{2}\,g \times 46{,}000 \times 1{\cdot}37 \times 10^{3} / 72$ = 89MPa. As the density of tungsten is approximately 19 × 10^{3}kg m^{-3}, such a slab should also contribute a mass per unit mirror area perpendicular to the Sun's rays of around 19 × 103 × 0.001 / 46,000 = 0·4g m^{-2}. This is not an excessive amount in relation to the probable mirror mass of, say, 5gm^{-2}. However, it is worth noting that unpublished estimates that the author has seen suggest that current solar thermal engine designs are considerably more massive than implied by this theoretical analysis, indeed they are probably even less close to what is theoretically achievable than are current concentrator designs, see next section.

https://doi.org/10.1017/S0001924000000956 Published online by Cambridge University Press

7.0 ENSURING THAT THE REQUIRED OPTICAL PRECISION IS ACHIEVED WITH THE MIRROR ARRANGEMENT

This is perhaps the biggest technical challenge facing the proposed vehicle design, since the very low mass solar sails now being developed are in effect merely very thin floppy sheets strung out in front of sunlight. The larger mirror (which forms the vast bulk of the mirror surface area) needs to be made from a very thin and therefore almost certainly non-rigid sheet, to minimise mirror mass. Given the degree of concentration involved, the angular accuracy of the main mirror positioning probably needs to be, say, 1 in 3,000 or better. The small second mirror is much less of a problem, as it should contribute relatively little to the overall mirror mass

Most previous investigators of solar-powered concentrators for astronautical purposes appear to have decided that it is impractical to achieve this level of positioning accuracy with a mirror akin to a solar sail. Instead they have typically proposed either refractive/diffractive arrangements or mirrored inflated concentrators. The former cannot typically be made very thin. The latter also typically have much higher masses per unit collector area. Using an inflatable collector at least doubles the mass per unit collector area (to surround the inflated region), and for a large collector the gas used within the inflated region can contribute significantly to the overall mass of the concentrator. The tension in the collector will also typically be inversely proportional to the radius of curvature of the inflated surface, which is likely to make it more difficult to achieve the desired accuracy with a thin film, unless its thickness varies across the collector surface (or more practically the sheet is likely to be thicker than it needs to be in some places to cater for more modest curvature in other places). The author has seen unpublished estimates which suggest that inflated concentrators might in practice have masses per unit area perpendicular to the Sun's rays circa 50 – 100 times more than those that appear to be achievable with a solar sail.

However, a presupposition such investigators appear to be making is that any solar-powered engine would necessarily be operating in an essentially zero *g* environment. This is potentially flawed logic, as it should be easier to achieve the desired optical positioning when a thin-film is experiencing effective accelerations closer to 1*g*. A simple way to justify this perhaps surprising claim is to apply an approximately uniform tension in all (tangential) directions to a sheet of some commercially available ultra-thin transparent sheet (e.g. kitchen cling-film). It adopts a well-defined (flat) shape that is sufficiently smooth to form a surprisingly good reflective image. So thin-film sheets such as those proposed for solar sails are likely to be able to achieve the desired level of optical precision as long as:

(a) The material out of which the sheet is made is reasonably inextensible;
(b) The sheet (or to be precise its mirrored surface) is sufficiently smooth;
(c) The sheet's natural shape matches that desired, i.e. if it were hypothetically put over a mould of exactly the desired shape then it would fit perfectly, with no kinks or slack; and
(d) The sheet is sufficiently tensioned throughout flight (probably with transverse and radial tension being approximately equal for any given point on the mirror surface throughout flight).

We analyse further point (*d*) as follows. Assume that the mirror is rotating around its axis of symmetry (the *x*-axis) with an angular speed $\dot{\theta}$ and the mirror is described as a surface using cylindrical polar co-ordinates (x, r, θ) where $y = r\mathrm{Cos}\theta$, $z = r\mathrm{Sin}\theta$.

We first consider the situation where there are many stanchions suitably positioned so that each part of the mirror is subject to a force from them per unit mirror area (cross-sectional area perpendicular to the *x*-axis) of $F(r,\theta) = (F_x, F_r, F_\theta)$. We assume initially that these forces are continuously distributed, although of course in practice there would be a finite (albeit possibly quite large) number of stanchions, so we would merely have a discrete approximation to this continuous ideal. Assume that the corresponding tensions within the mirror (per unit cross-sectional area) are $T(r,\theta) = T_r$, T_θ in the plane of the mirror, see Fig. 12.

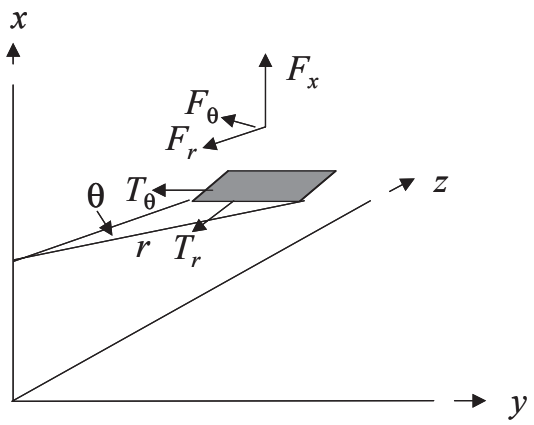

Figure 12. Forces on a small part of the larger mirror.

In the absence of thrust, the vehicle would be in free-fall. If in addition $F(r,\theta) = (0,0,0)$ and $\dot{\theta} = 0$ then there would be no tension within the mirror and it would be completely floppy. If we assume as above that the vehicle ejects propellant along the positive *x*-axis and if we arrange for $F_\theta = 0$ then all of the forces on the mirror are rotationally symmetric. We could in principle have the mirror made up of several concentric annuli with transmission mechanisms between them that allow different annuli to rotate at different speeds, but this would add complexity and mass to the overall arrangement, so we assume that $\dot{\theta}$ is constant for all r although not necessarily constant for all t. The equations of motion satisfied by the mirror therefore become:

$$-F_x r + c\frac{d\left(T_r r\mathrm{Cos}a\right)}{dr} = \frac{c\rho}{\mathrm{Sin}a} r\bar{g} \qquad \ldots (11)$$

$$F_r r + c\left(\frac{d\left(T_r r\mathrm{Sin}\,a\right)}{dr} - \frac{T_\theta}{\mathrm{Sin}\,a}\right) = -\frac{c\rho}{\mathrm{Sin}\,a} r^2\dot{\theta}^2 \qquad \ldots (12)$$

We first note that ideally we would have constant ratios between F_x, F_r, T_r and T_θ for all t (and hence we would have the angle, $\beta(r,t) = \mathrm{Arctan}(F_r/F_x)$, that each stanchion would make to the *x*-axis, were there to be merely one stanchion for each mirror element, also independent of t). This can be achieved by keeping $\dot{\theta}^2$ proportional to $\bar{g}$, i.e. s constant, perhaps by ejecting a small proportion of the propellant in a manner that creates a torque that when transmitted to the mirror increases or reduces its rotational speed.

We next note that it is possible to come up with plausible arrangements that do potentially keep the mirror tensioned in the manner indicated above. Reverting to the iterative notation used previously, focusing on the part of the mirror where $m_{1,y}$ is positive (and starting at 1), and scaling the overall mirror size so that its overall radius is r_0 we have:

$$\frac{F_x}{c\bar{g}} = F_1\frac{T_r}{r_0\bar{g}} + F_2\rho + F_6\frac{T_r'}{r_0\bar{g}}$$
$$\frac{F_r}{c\bar{g}} = F_3\frac{T_r}{r_0\bar{g}} + F_4\frac{T_\theta}{r_0\bar{g}} + F_5 r_0\rho s + F_7\frac{T_r'}{r_0\bar{g}} \qquad \ldots (13)$$

https://doi.org/10.1017/S0001924000000956 Published online by Cambridge University Press

Table 6
Values of F_1, …, F_7 arising from use of $q_1 = 1$, $q_2 = -0{\cdot}3$, $sgn(h) = -1$ for various $m_{1,y}$

$m_{1,y}$	F_1	F_2	F_3	F_4	F_5	F_6	F_7
0·999	–1·43	–1·05	–1·51	1·05	–1·05	0·31	–0·95
0·99	0·04	–1·05	–1·05	1·06	–1·04	0·31	–0·95
0·95	0·48	–1·05	–0·95	1·11	–1·00	0·31	–0·95
0·90	0·57	–1·05	–0·99	1·17	–0·94	0·30	–0·95
0·81	0·62	–1·04	–1·11	1·29	–0·84	0·28	–0·96
0·70	0·66	–1·03	–1·31	1·47	–0·72	0·24	–0·97
0·62	0·68	–1·02	–1·51	1·66	–0·63	0·22	–0·98
0·52	0·69	–1·02	–1·81	1·94	–0·53	0·19	–0·98
0·41	0·70	–1·01	–2·31	2·42	–0·42	0·15	–0·99
0·30	0·72	–1·01	–3·26	3·34	–0·30	0·11	–0·99

Table 7
F_x, F_r and hence F_T as multiples of $c\bar{g}$ (and hence angle, β, that a single cross-stanchion should make to the x-axis) needed in order to achieve uniform tension in larger mirror for a hypothetical mirror example

$m_{1,y}$	$F_x/c\bar{g}$ (×10³)	$F_r/c\bar{g}$ (×10³)	$F_T/c\bar{g}$ (×10³)	β(°)
0·999	–17·6	–23·3	29·2	52·9
0·99	–10·3	–20·8	23·2	63·6
0·95	–8·1	–19·2	20·8	67·1
0·90	–7·6	–17·9	19·4	66·9
0·81	–7·3	–15·9	17·5	65·4
0·70	–7·0	–13·6	15·3	62·7
0·62	–6·9	–11·9	13·8	60·1
0·52	–6·7	–10·0	12·1	56·1
0·41	–6·6	–7·9	10·3	50·2
0·30	–6·5	–5·7	8·6	41·2

where $$F_1 = \frac{m_{1,y}(k+1)\mathrm{Cos}\left(a_1(k+1)\right) - m_{1,y}(k)\mathrm{Cos}\left(a_1(k)\right)}{m_{1,y}(k)\left(m_{1,y}(k+1) - m_{1,y}(k)\right)}$$

$$F_2 = -\frac{1}{\mathrm{Sin}\left(a_1(k)\right)}$$

$$F_3 = -\frac{m_{1,y}(k+1)\mathrm{Sin}\left(a_1(k+1)\right) - m_{1,y}(k)\mathrm{Sin}\left(a_1(k)\right)}{m_{1,y}(k)\left(m_{1,y}(k+1) - m_{1,y}(k)\right)}$$

$$F_4 = \frac{1}{m_{1,y}(k)\mathrm{Sin}\left(a_1(k)\right)}$$

$$F_5 = -\frac{m_{1,y}(k)}{\mathrm{Sin}\left(a_1(k)\right)} \quad F_6 = \mathrm{Cos}\left(a_1(k+1)\right)$$

For mirror layouts as per Figs 9 and 10 then F_1, …, F_7 are as per Table 6 for a range of well spread out values of $m_{1,y}$. We note that in the situation where $T_r = T_\theta = T_a$ and T_a is constant for all r (for a given t), i.e. F_6 and F_7 can be ignored, the following apply:

(*i*) For small T_a, the terms in F_3 and F_5 predominate, and as we might expect have the desired signs, i.e. they involve the wires pulling the mirror along in the direction of the negative x-axis and radially inwards.

(*ii*) For any given T_a, the terms in F_3 and F_5 still predominate for sufficiently large r_0. This means that sufficient tension to achieve a smooth reflective surface can always in principle be achieved as long as r_0 is large enough.

If, say, $\rho = 10 \times 10^3 \mathrm{kgm}^{-3}$, $T_a/\bar{g} = 1\mathrm{MPa}$ (so T_a is roughly 8 – 14 MPa during flight), $\dot{\theta}^2/\bar{g} = 0{\cdot}01$ and $r_0 = 200\mathrm{m}$ then $F_x/c\bar{g}$, $F_r/c\bar{g}$ and $F_t/c\bar{g}$ (and if there is a single stanchion per mirror area element, β) are as per Table 7 for various values of $m_{1,y}$. The above values of ρ, r_0 etc. have been chosen to be akin to those that might arise when lifting a modest payload into orbit. We note that F_x and F_r have the desired signs as per (*i*) for all relevant $m_{1,y}$. As long as the stanchions are sufficiently close together the tension will vary only a little in the regions between stanchions, making it possible in principle to achieve the desired level of optical accuracy. Some cross buttressing might also be desirable, to limit vibration of the mirror during flight, unless a particularly smooth acceleration is delivered by the engine.

The reason that it is more difficult to achieve the desired position accuracy in a very low or zero g environment is that $\bar{g}$ is then several orders of magnitude smaller than the circa 8 – 14ms^{-2} applicable in the above proposed pre-orbital trajectory. We can still ensure that F_5 predominates in the calculation of F_r by making s large enough. But in the calculation of F_x we find that F_1 generally has the 'wrong' sign and hence (for small $\bar{g}$) F_x is in the positive rather than negative x direction.

Overcoming this undesirable feature when $\bar{g}$ is small is likely to require an impractically large r_0 or some sort of boom that allows us to apply a force to the mirror in the positive x direction. Such a boom adds mass. Alternatively, we would need to use an inflatable concentrator (the pressure within the inflated part then providing the necessary force in the positive rather than the negative x direction).

We might seek to dispense with most of the stanchions and instead include concentric wires within the mirror surface that mitigate tension differentials that would otherwise arise across the mirror surface. T_r' would then be non-zero in each region within consecutive concentric wires, and at each edge of each such region we would, in effect, be able to reset T_r and T_θ to be closer to what we would like by choosing a suitable tension for the wires themselves. However, it would then be difficult to avoid having some stanchions scattered across the mirror as if they were all attached to the outer rim of the mirror then they would in aggregate provide too much centripetal acceleration, causing the rim to bend back in on itself.

The above comments apply, in broad terms, to any optical concentrator. Suppose that we have a concentrator with focal length Y. To first order, near its optical axis, $\mathrm{Cos}a(r) = r/Y$ and $\mathrm{Sin}a(r) = 1$ so to first order we have:

$$\frac{F_x}{c\bar{g}} = \frac{1}{Yr\bar{g}}\frac{\mathrm{d}(T_r r^2)}{\mathrm{d}r} - \rho \;\Rightarrow\; \frac{F_x}{c\bar{g}} = \frac{1}{Y\bar{g}}\left(rT_r' + 2T_r\right) - \rho \qquad \ldots (14)$$

$$\frac{F_r}{c\bar{g}} = -\frac{1}{r\bar{g}}\left(\frac{\mathrm{d}\left(T_r r\right)}{\mathrm{d}r} - T_\theta\right) - \rho rs$$
$$\Rightarrow \frac{F_r}{c\bar{g}} = -\frac{1}{r\bar{g}}\left(rT_r' + T_r - T_\theta\right) - \rho rs \qquad \ldots (15)$$

So if we want $T_r' \approx 0$ whenever $F_x \geq 0$ (which would be desirable in any region where there wasn't a stanchion or if we wish to avoid a boom or inflated structure) we ideally want $Y \geq T_r/(2\rho\bar{g})$. Practical concentrators are likely to have dimensions not hugely different to their focal length, so we conclude that ideally their sizes should also be of the order of at least $T_r/(2\rho\bar{g})$.

Ideally, we would also want $T_r \approx T_\theta$ and $T_r' \approx 0$ whenever $F_r \approx 0$ in any region where there wasn't a stanchion or a tension wire, i.e. for $\dot{\theta}^2$ to be small in relation to $T_r/(2\rho r^2)$. But if $\dot{\theta}^2$ is too small then we would have T_θ negative at the mirror rim, since F_r needs to be negative there for a practical stanchion configuration, see earlier.

8.0 OTHER PRACTICAL ISSUES

Figure 11 includes an exhaust guide designed to keep the propellant from fouling the mirror and *vice versa*. This is desirable because plume divergence can be very large in space. With a mirror layout as

https://doi.org/10.1017/S0001924000000956 Published online by Cambridge University Press

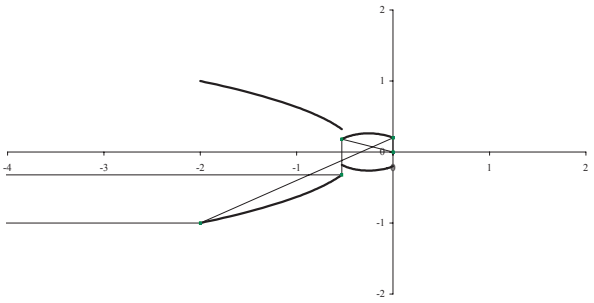

Figure 13. Mirror layout arising from $q_1 = -2$, $q_2 = 0{\cdot}2$ and sgn(h) = 1.

per Fig. 9, the inner edge of the light rays travel along a line from circa (–0·08, 0·03) to (1·16, 0·30), which crosses the y-axis at (0, 0·04). If we assume that the exhaust guide is conical, forming the surface of revolution around the x-axis of the line segment from (0, 0·04) to (1·16, 0·30) then it would have a surface area that was about 43% of the overall collector area. It would therefore itself need to be made of an ultra-low mass material. If $q_2 = -0{\cdot}1$ not –0·3 (but q_1 is still 1 and sgn(h) = –1) then the radius of the hole in the middle of the mirror reduced by a factor of three. This reduces the surface area of the exhaust guide to only about 12% of the collector area. Such a design still has acceptable optical characteristics; its aperture factor rises to 99%, its mirror surface area factor is 1·019 and its aberration factor is 0·060.

Near the rocket nozzle itself, the expelled propellant would of course be at a high temperature, so this part of the exhaust guide is unlikely to be able to be made of the same material as the mirrors. But this is where the exhaust guide is narrowest, so it is also the part of the guide where there is least problem in its mass per unit area being higher. Indeed, one can think of the exhaust guide as in effect a very long extension to the rocket nozzle, which should facilitate further adiabatic cooling as the ejected propellant travels along it. This might increase the overall energy efficiency of the engine compensating in part for the extra mass needed near to the rocket engine itself.

Ejecting the propellant along the positive x-axis through the hole in the main mirror means that the thrust generated by the propellant ejection is likely to pass through the centre of gravity of the vehicle (which is likely to lie along the x-axis given the symmetric shape of the main mirror). Keeping the thrust always about parallel to the axis of rotation should aid flight stability. However, this also means that the positive x-axis would be in the opposite direction to the Sun. This means that the arrangement would operate most effectively only when the Sun was at a suitable inclination (i.e. approximately 45° to the vertical). Typical flight times would be sufficiently short in any pre-orbital phase that the change in the inclination during flight would not be particularly large in this context, so we can overcome this issue within the pre-orbital phase by launching at suitable times of day (and within certain, albeit relatively wide, latitudes of the equator). Once orbit is reached, a more leisurely approach can be adopted, e.g. waiting until a part of the orbit is reached when the Sun is suitably positioned.

There are also constraints on the payloads that such a vehicle could lift into orbit. For example, suppose that the mirror weighs Mkg and that the wires joining the mirror to the main engine are on average at a 45° angle to the axis of symmetry. The maximum acceleration experienced by the mirror might be approximately $\sqrt{2}g$. The force (parallel to the axis of symmetry) that the wires joining the engine to the main mirror would therefore need to apply to the mirror would be approximately $10\sqrt{2}\ M$kgms^{-2}. Since the surface area of the mirrors is, say, $M/0{\cdot}005\text{m}^2 = 200\text{M}$, the length of these wires might be of the order $\sqrt{2\times 200M} = 20\sqrt{M}$ m. If we assume that the wires are made of tungsten with a tensile strength of 3,500MPa and a density of 19×10^3kg m^{-3} then the mass of the wires would then be at least approximately $\text{M}^{3/2} \times 10\sqrt{2} \times \sqrt{2} \times 20 \times (19 \times 10^3)/(3{\cdot}5 \times 10^9) = 0{\cdot}0022\text{M}^{3/2}$kg, and hence would be at least as massive as the mirror if M were greater than circa 210,000kg.

If we wished merely to use solar power for orbital transfer then the practical issues referred to above can be circumvented by using a different aplanatic two-mirror layout, with, for example q_1 negative, q_2 positive (between 0 and 1) and h positive[6]. Figure 13 shows such a layout, if iterated to its extremities, derived from $q_1 = -2$, $q_2 = 0{\cdot}2$ and $sgn(h) = 1$. The lighter lines are again cross-sections of the mirrors themselves, and the darker lines are the paths of light rays from the object to the image passing through extremities of the available iterative process. Both mirrors are now 'in front of' the focal point so propellant can now be expelled in a wide range of directions without fouling the mirrors. This layout has an effective aperture factor of 90% and an aberration factor of 0·02, i.e. not dissimilar to the ones described earlier. Unfortunately, it has a mirror surface area factor of 2·86, i.e. its mass would be about 2·8 times that of the mirror arrangement shown in Fig. 8. It would also need a boom to hold the mirror in tension parallel to the x-axis (further increasing the mass of the arrangement) as well as needing to be rotated around the x-axis to provide the necessary tension in the mirrors parallel to the y and z-axes. If all that is required is a leisurely approach to orbital transfer akin to the 15 – 30 days proposed for the SOTV then the extra mass per unit collector area perpendicular to the Sun's rays would be less problematic, although the collector arrangement would then be much less effective for any potential subsequent solar sail use.

9.0 OTHER COMMENTS

Hopefully this paper will stimulate others to consider further the potential for solar-powered space flight. When doing so, it is worth noting that:

(a) There appears to be a big disparity between currently available component performance for solar-powered thrust in space and what ought theoretically to be achievable. Without some bridging of this gap, usage of any form of solar-powered thrust in space may remain limited.

(b) Longer-term, if component performance can reach closer to what ought theoretically to be achievable then solar-powered propulsion may have a bright future. With big enough component improvements, solar-powered space propulsion should become practical for late pre-orbital, orbital transfer and post-orbital flight, and particularly when a flight involves all three, since the same collector arrangement can be used in all three of these stages.

(c) The ideal size for ultra-low mass optical concentrators for use in space is probably of the order of at least $T/(2\rho\bar{g})$ where T is a tension sufficient to keep the concentrator taut but not so great to cause inelastic deformation, $\bar{g}$ is the effective acceleration being generated by thrust and ρ is the average density of the thin film. Vehicles aiming to use solar power for late pre-orbital flight seem likely to be broadly consistent with this design characteristic. Current astronautical optical concentrators, being quite small and typically designed to operate in essentially zero g environments, are typically too small to satisfy this design criterion.

REFERENCES

1. KAYE, G.W.C. and LABY, T.H. *Tables of Physical and Chemical Constants*, 15th edition, Longman Scientific & Technical.
2. NASA solarsail.jpl.nasa.gov/introduction/design-construction.html.
3. Team Encounter www.teamencounter.com/starship/spacecraft_sailcraft .asp.

https://doi.org/10.1017/S0001924000000956 Published online by Cambridge University Press

4. KLEIN, M.V. and FURTAK T.E. *Optics*, 1986, John Wiley & Sons.
5. KEMP, M.H.D. *Optical Imaging Device Design for Solar Powered Flight and Power Generation*, 2003, PCT Patent Application PCT/GB2003/004516.
6. KEMP, M.H.D. *Ultra-high Resolution Imaging Devices*, 2001, PCT Patent Application PCT/GB2001/01161.
7. US National Research Council Committee on Thermionic Research and Technology. *Thermionics Quo Vadis? An Assessment of the DTRA's Advanced Thermionics Research and Development Program*, 2001, National Academy Press.
8. WINSTON, R. Nonimaging optics, *Scientific American*, March 1991.

https://doi.org/10.1017/S0001924000000956 Published online by Cambridge University Press